Organic compounds for solid state luminescence enhancement/aggregation induced emission: a theoretical perspective

Michele Turelli, Ilaria Ciofini, Qinfan Wang, Alistar Ottochian, Frédéric Labat, Carlo Adamo

Organic compounds for solid state luminescence enhancement/aggregation induced emission: a theoretical perspective

Michele Turelli[*1], Ilaria Ciofini*[*1], Qinfan Wang[1], Alistar Ottochian[1], Frédéric Labat[1], Carlo Adamo*[*1,2]*

[1]*Chimie ParisTech, PSL University, CNRS, Institute of Chemistry for Life and Health Sciences, Theoretical Chemistry and Modeling Team, 75005 Paris, France;*

[2]*Institut Universitaire de France, 103 Boulevard Saint Michel, F-75005 Paris, France.*

Abstract:

Organic luminophores displaying one or more forms of luminescence enhancement in solid state are extremely promising for the development and performance optimization of functional materials essential to many modern key technologies. Yet, the effort to harness their huge potential is riddled with hurdles that ultimately come down to a limited understanding of the interactions that result in the diverse molecular environments responsible for the macroscopic response. In this context, the benefits of a theoretical framework able to provide mechanistic explanations to observations, supported by quantitative predictions of the phenomenon, are rather apparent. In this perspective, we review some of the established facts and recent developments about the current theoretical understanding of solid-state luminescence enhancement (SLE) with an accent on aggregation-induced emission (AIE). A description of the macroscopic phenomenon and the questions it raises is accompanied by a discussion of the approaches and quantum chemistry methods that are more apt to model these molecular systems with the inclusion of an accurate yet efficient simulation of the local environment. A sketch of a general framework, building from the current available knowledge, is then attempted via the analysis of a few varied SLE/AIE molecular systems from literature. A number of fundamental elements are identified offering the basis for outlining design rules for molecular architectures exhibiting SLE that involve specific structural features with the double role of modulating the optical response of the luminophores and defining the environment they experience in solid state.

Corresponding authors: michele.turelli@chimieparistech.psl.eu; ilaria.ciofini@chimieparistech.psl.eu; carlo.adamo@chimieparistech.psl.eu

1. Introduction

Organic compounds hold an incredible potential for application in virtually all key technological fields defining of the current era[1,2]. The complexity and structural variety that they can achieve is well exemplified by the molecular machinery that powers and shapes living matter. Beside astonishing in itself, the complexity of biomolecules is specifically associated with the fulfillment of particular functions, engineered by evolution as intricate combinations of responses to different possible stimuli, like electromagnetic radiation, mechanical stress or changes in chemical environment.

This tunable responsiveness is precisely the reason behind the huge technological appeal of organic materials and it is mainly ascribable to two essential characteristics: the propensity to form complex π-conjugated structures and the possibility to include 'heteroatoms', most commonly O, N, S, P, B and Si, in arbitrarily large stable compounds to modify their electronic properties. These two ingredients together, ensure a remarkable 'plasticity' of the electronic structure around the nuclear configuration that is at the basis of the wide spectrum of behaviors of carbon-based materials. Of particular interest are electric and optical responses that can be exploited for application in the ever-expanding field of organic optoelectronics[3]. Thanks to their peculiar structural and electronic features, organic compounds usually possess a very rich photophysics that is expressed as multiple absorption in the UV-vis range and a luminescent emission that may sometime be of composite nature - for example, for compounds manifesting anti-Kasha behavior[4] or thermally activated delayed fluorescence (TADF)[5,6] among others - and that carries vibronic signatures associated with the molecular structure[7]. Luminescence has been the subject of much focus recently as its quantitative prediction and experimental control entail an understanding of many molecular processes at the excited state that often carry a strong dependence on the local environment of the luminescent unit. This environment is determined by a number of factors such as aggregation state, complexation with solvent, or experimental conditions such as temperature or pH[8-15]. This dependence may result in a faint emission (especially for what concerns phosphorescence) in the range of conditions, i.e., solid phase, required for most technological applications, a phenomenology that renders otherwise appealing materials very difficult to exploit. This is especially true for many polyaromatic hydrocarbons that in solution exhibit pronounced luminescence but once aggregated undergo a strong emission quenching[16]. This issue can be seen as a drawback brought forth by the same features that allow these π-conjugated chromophores to express such a complex behavior in the first place. Indeed, efficient deexcitation channels for excited states can be present due to the strong coupling of electronic and vibrational degrees of freedom of the molecule that may involve the whole molecule or some of its parts. The main cause of the observed photoluminescence quenching in the aggregated state can be traced to excitation energy transfer[17-19] and the subsequent action of dissipation processes mediated by the supramolecular structures found in concentrated solutions or in aggregates and determined by weak intermolecular forces, a phenomenon known as *aggregation-caused quenching* (ACQ)[20].

However, although less frequent, an opposite behavior observed for a few classes of compounds has received in recent years a lot of attention. While non-luminescent in solution, these compounds express enhanced emission in aggregated phase. This *solid-state luminescence enhancement* (SLE) has been reported and investigated systematically for a number of compounds during the last century[21,22] but its study has received a considerable boost since the same macroscopic phenomenon has been reported for a particular kind of compounds under the name of *aggregation-induced emission* (AIE) and it has since been recognized for several other molecular families with different magnitudes[16,23,24]. If the enhanced luminescence in solid state has a similar macroscopic manifestation for all compounds, i.e., an increase of photons emitted over absorbed ones, its molecular origins, despite the presence of some common features, can be as varied as the classes of molecules displaying it[25]. From this fact comes the considerable difficulty of developing and choosing apt theoretical tools to describe them.

It remains, nonetheless, of extreme importance to provide a better understanding of the observed macroscopic luminescence enhancement to open the way at the rational and tailored design of new compounds. In this work, after a general description of the SLE/AIE phenomena and of the possible theoretical approaches enabling its modeling, selected cases representative of the different classes of compounds and mechanisms at work will be described in order to give a clear picture of the current state of the art.

2. SLE/AIE: basic principles and underlying mechanisms

A general framework for the interpretation of the mentioned phenomena may be given starting from the description of single photoactive units taken as fundamental building blocks. The relevant process to describe is then the aggregation and organization of a number of these building blocks resulting from noncovalent interactions. These last comprise all those residual interactions between electronic densities of the different molecular units that either have classical equivalents (e.g., dipole, quadrupole) or are strictly quantum in nature (e.g., induced dipoles, London or dispersion forces). These types of interactions are usually ‘weak’ so that the effects of aggregation on the physical properties of the molecular units are mainly reflected in -usually- small conformational changes caused by packing and in the emergence of an anisotropic polarizing environment determined by the aggregated medium[26,27].

The presence of a large number of independent molecular units interacting noncovalently in solid state is at the basis of the complex phenomenology ranging from ACQ to SLE/AIE. Noncovalent interactions are associated with particularly shallow potential energy profiles that govern supramolecular organization. These profiles feature many competing minima corresponding to different molecular arrangements that coexist in real-life samples and that may be populated or not depending on the experimental conditions[28]. This situation results in a vast array of possible configurations in the solid, that includes the disordered morphologies of amorphous aggregates alongside the ordered ones of multiple crystalline structures due to polymorphism[29-31]. The presence of many solid-state molecular arrangements introduces another variable that may further modulate the emissive behavior and that

sometimes results in different aggregated morphologies of the same compound displaying different photoluminescence[32-35].

The renewed boost to the study of materials showing AIE, also known as AIEgens, has resulted in the development of a conspicuous number of experimental applications concerning novel sensing and imaging techniques[36-44] but also other crucial technologies like organic light emitting diodes (OLEDs) or luminescent solar concentrators (LSCs)[45-48].The experimental community has been rapidly followed by the theoretical one, that has found in the AIE phenomenon a fertile playground as it includes a number of physical processes whose interpretation is highly relevant also for the advancement of theoretical approaches. Among these, the prominent role that conical intersections (CIs) are thought to play in the photophysical response of AIE compounds or the previously mentioned description of noncovalent interactions in the modeling of complex chemical environments.

Despite the remarkable advances in the quest to clarify the main features of the AIE phenomenon[16,49,50], the many factors involved make it difficult to predict whether a compound will exhibit SLE just by looking at its chemical formula, to the extent that two similar compounds might exhibit completely different behaviors[51-55].

In this context, computational protocols able to perform an assessment of these determining factors or an evaluation of specific descriptors would serve well an experimental community keen on the possibility of enhancing and customizing AIEgens performances for specific functions via computationally assisted chemical design. To this aim, the most pressing issue is to gain the modeling ability of revealing the eventual luminescence enhancement in those complex environments commonly found in technological applications, e.g., polymer matrices[56-60], in a simple way and while maintaining the computational costs as low as possible, without the need of performing for each system the expensive analyses that have been so far fundamental in clarifying some major aspects of the processes resulting in AIE[61-62].

As already mentioned, the SLE/AIE phenomenon consists in the environment modulation of the photophysical units' behavior in condensed phase that becomes apparent when comparing the photoluminescence of isolated fluorophores in diluted solution ($< 10^{-3}$ M) to the one of aggregated fluorophores assembled in amorphous structures or small crystallites depending on the system under investigation. Therefore, any theoretical approach that aims at predicting the SLE character of a molecule from its structure, must include a method for the calculation of the electronic structure and its response in presence of an additional model reproducing the environment. This model is expected to provide a description of the molecular surroundings capable of reproducing the main environmental effects while remaining simple and with a reduced number of parameters and degrees of freedom. On top of this, the physical quantities predicted are also required to provide a link to the typical observables that are measured in experiments. In this regard, the main quantitative observable that serves as a fingerprint for the SLE/AIE phenomenon is the *photoluminescence quantum yield* ϕ_{PL}, defined simply as the ratio between photons emitted by the irradiated sample over absorbed ones. Mathematically, this

quantity can be expressed in terms of two rate constants describing the probability over time for the electronic excitation to decay with or without the emission of a photon:

$$\phi_{PL} = \frac{k_r}{k_{nr}+k_r} \quad (1)$$

Here, k_r is the rate constant for the process involving a molecule in an excited state - either a singlet or a triplet, usually S_1 or T_1 according to Kasha's rule[63] – that deexcites radiatively, while k_{nr} represents the same quantity for the non-radiative case. k_{nr} includes multiple terms that encode all major processes that deplete the population of the excited state other than photon emission. All these processes come down to a redistribution of electronic energy to rotational and vibrational degrees of freedom of molecule itself or belonging to the environment. This redistribution might be realized within the molecular system through nonadiabatic coupling, eventually assisted by electronic processes like intersystem crossing that extends the excited states lifetimes, or via interactions with the surroundings, directly through collisions or aided by more complex phenomena, such as excitation energy transfer or the activation of reactive channels. The photoluminescence quantum yield ϕ_{PL} defined in eq.1 includes both fluorescent and phosphorescent emission. By tracking its changes along the physical and chemical evolution of the sample of interest, it is possible to reveal a host of phenomena among which those determined by the aggregation state.

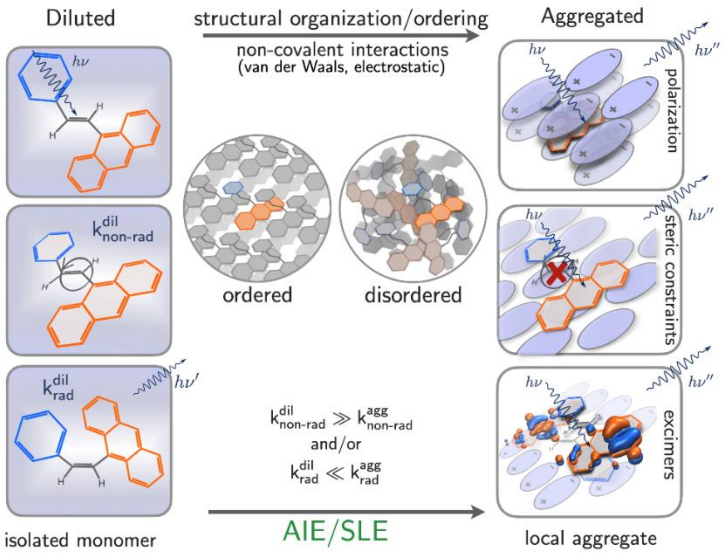

Figure 1. Schematic representation of the difference in molecular response at the excited state between diluted and aggregated phases leading to observed AIE/SLE phenomena.

Additionally, the same expression in eq.1 also provides another convenient picture to interpret the SLE phenomenon in more general terms. Quantum yield results from the competition of radiative and non-radiative deexcitation processes, hence the increase in photoluminescence recorded for AIEgens can originate from two limiting scenarios, (i) a decrease of k_{nr} or (ii) an environment modulated increase of k_r . The generality of these scenarios further underlines how the macroscopic phenomenon of SLE/AIE actually encompasses a variety of possible mechanisms that simply need to realize one or a combination

of both conditions presented. Conditions that are determined by the complex balance and tuning between intermolecular and intramolecular interactions typical of organic solids, as schematically depicted in Figure 1.

Despite this potential diversity, a consensus on the most common molecular mechanism underlying SLE has emerged, mainly thanks to the invaluable input of a prolific experimental community that has generated a wealth of observations offering the fundamental basis for a solid theoretical understanding[16,24,49,64-66]. This mechanism essentially ascribes the increased luminescence to the first outlined scenario, according to which the decrease of non-radiative rates is due to the action of the intermolecular forces introduced by molecular packing in the aggregates. This picture identifies the structural constraints emerging in the solid-state environment as the cause for the restriction of the intramolecular motions mediating the non-radiative decay. Indeed, most AIEgens reported so far carry bulky functional groups that participate in the optical response and whose substantial reorganization during structural relaxation at the excited state plays a fundamental role in promoting the non-radiative decay. However, this model, commonly referred to as *Restriction of Intramolecular Motions* (RIM)[55,65], only partially captures the phenomenon. The environment can also induce a significant polarization of the chromophores resulting in a net enhancement of fluorescence in presence of (rather) limited geometrical constrains[66].

In general, a non-radiative deexcitation occurs whenever the adiabatic potential energy surfaces (PESs) of two states are connected. This connection can either happen at a so-called conical intersection (CI), where the two adiabatic surfaces intersect and the excited and ground electronic states become degenerate, or through a perturbation term in the Hamiltonian allowing the coupling of the electronic and vibrational states, and thus conversion via the transfer of the energy to the multitude of vibrational degrees of freedom.

For many AIEgens, it is only the involvement of a CI that can explain the extremely fast process (in the order of a few picoseconds[49]) of the deexcitation, as it has been confirmed by a number of theoretical studies on various systems[50,67,68]. When the CI is the most plausible route for the non-radiative decay in solution, then the enhanced solid-state luminescence is said to be due to a *Restricted Access to the Conical Intersection* (RACI) that happens in the aggregated phase. If the deexcitation is mediated by a coupling involving the nuclear kinetic energy term[49,69-71] then the mechanism is more likely of type RIM and it can be treated with standard perturbation theory, i.e., Fermi's golden rule (FGR).

In summary, the pronounced geometrical reorganization typical of most AIEgens causes the system to access regions of the excited PES far from the minimum where these processes are particularly effective in dissipating the excitation energy and in bringing the system back to the electronic ground state.

3. Modeling SLE/AIE: issues to address and approaches

Independently from the underlying mechanism, it is clear that the minimal requirement for a computational approach aimed at the description of SLE/AIE phenomena is the ability to describe, with

comparable accuracy, the photophysical properties of an organic compound in solution and in solid phase. For the typical organic fluorophore, both these environments affect the molecular electronic structure and its response via the modulation of three parameters: (i) molecular geometry, (ii) the local environment polarizability, i.e., how the electronic densities of neighboring molecules respond to and influence the local excitation, and (iii) the eventual formation of excimers that determines the emergence of new optical units with photophysical properties distinct from those of the isolated phosphors.

Let us first consider the case of excimer formation[72,73] (even beyond a molecular dimer) upon aggregation. This phenomenon has long been recognized to have a leading role in the emergence of additional photoluminescence features in condensed phases for many systems[74-77]. Commonly, isolated molecules are taken as main photophysical units, because at standard experimental conditions, static and dynamic disorder tend to disrupt long-range quantum coherence localizing the excitation. For AIEgens, this assumption holds for those characterized by bulky moieties for which the optimal molecular packing does not allow distances between active moieties that are small enough to promote the excimer formation, yet examples of AIEgens where the excitation extends beyond a single unit are not rare[79-81].

As mentioned above, beyond the specific phenomenon of SLE/AIE, the formation of excimers is an important process that is frequently encountered in the optical behavior of organic chromophores. The formation of excimers determines both absorption and emission properties for many compounds that have long been studied precisely for this reason[82] and that can be described rather well with current theoretical approaches[83-86]. The case of perylene bisimide (PBI) derivatives is particularly fitting to the present discussion by virtue of the many behaviors PBI dyes display depending on the substituents on the imide groups. In a recent study[87], in which the experimental characterization has been accompanied by a computational analysis, PBIs functionalized with two small methyl moieties bonded to the imide nitrogen atoms (P-red179, from the nomenclature in ref. 87, see Figure 2), have been dispersed in a heterogeneous matrix, predominantly composed of low-density polyethylene, to form films with different P-red179 concentrations and a possible application in NIR reflecting coatings[88].

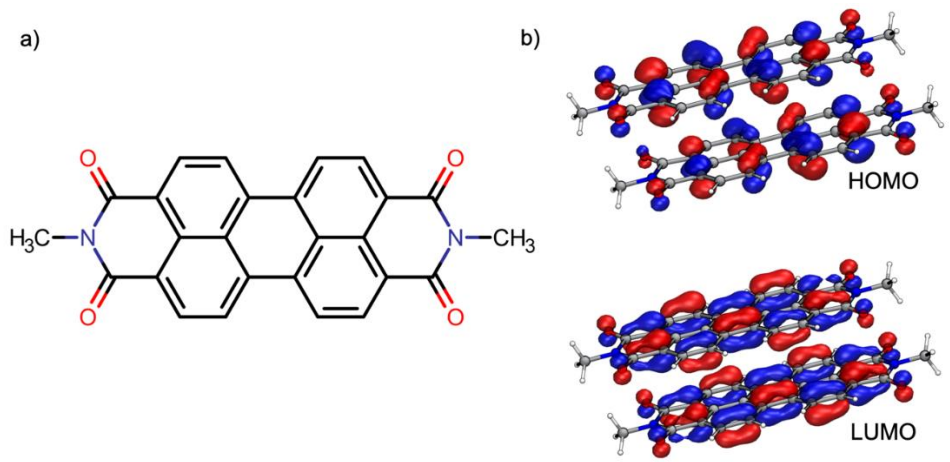

Figure 2. a) Sketch of pigment red 179 (P-red179) from ref. 87 and b) depiction of the frontier Kohn-Sham orbitals associated with the low energy absorption peak of the isolated dimer in solution (acetonitrile, PCM). The delocalization over both molecular structures signals the excimer response.

Samples of these composite films have been optically characterized with vis-NIR spectroscopic techniques. In addition, the absorption of P-red179 systems has been also investigated via theoretical calculations. Given the presence of rather large aggregates (in the μm scale) and the evidence of XRD spectra with sharp peaks consistent with the presence of ordered structures within the matrix, the analysis has focused on the chromophores in the crystalline environment. This choice appears to be reasonable also in view of the propensity of P-red179 units to stack due to the π-π interactions of PBIs conjugated cores. The absorption of a number of optical units (monomer, dimer, trimer and tetramer) has been simulated in the presence of an electrostatic embedding model for the crystal environment. Two peaks have been identified at different energies, i.e., 2.04 and 2.77 eV, with good agreement with the maxima reported experimentally. Crucially, the two maxima can be clearly attributed to the absorption peaks of the monomer and dimer models, with the results for trimers and tetramers extracted reporting essentially the same transitions on monomers and dimers in the larger assembly.

The picture drawn from the computational data indicates that the optical behavior of P-red179 is largely determined by the formation of excimers that, for PBI derivatives, emerge under all the relevant experimental conditions, stressing how their role is sometimes dominant in the optical response.

Considering now the 'simpler' case when the photoactive unit is the same both in solution and in the solid phase, it is necessary to access the theoretical tools enabling an accurate evaluation of its emission properties in both environments.

The inclusion of solvent effects on spectroscopic properties of organic compounds has been the subject of extensive research and accurate models have been developed and benchmarked especially in conjunction with quantum chemical methods rooted in density functional theory (DFT)[89-95]. Very often, systems in solutions are treated applying implicit solvent models, such as the *polarizable continuum model* (PCM)[96,97], or the *conductor-like screening model* (COSMO)[98,99]. These models ensure an effective description of the mutual polarization of solute electronic density and the solvent that produces often sizable shifts of transition energies (up to ±0.3 eV[27]) and modifications of the excited-state relaxed geometries with respect to the gas phase. Thanks to these approaches, it is possible to derive an average picture of the solution environment that has been proven to accurately reproduce the modifications induced on the solute's electronic structure in terms of excitation energies[90,93]. At the same time, these models have intrinsic shortcomings in the description of the constraining effects that viscous solvents exhibit on the structures of the chromophores. These constraints are linked to the steric hindrance of solvent molecules and sometimes result in increased quantum yields even for AIEgens diluted in these solvents[100-104]. These effects might be retrieved when considering explicit solvent models where a number of solvent molecules are included explicitly with actual atomistic detail, at the cost of an increased computational load. To reduce this cost, calculations on these systems can be carried out employing hybrid models, labelled as QM/MM, where quantum descriptions for the photoactive solute,

eventually including the first or few solvation shells, are combined with a molecular mechanics one for the rest of the explicit solvent molecules.

One notable example of this modeling approach is the one reported in ref. 105. Here, a range of different methods to include the solvent environment are coupled with a quantum chemical description (TD-DFT) to predict absorption and fluorescence maxima for uracil in aqueous solution. The experimental behavior observed for this molecule in gas phase and in aqueous solution indicates the presence of two states with a dark and a bright character that are understood to be a $n \rightarrow \pi^*$ and a $\pi \rightarrow \pi^*$ excitations, respectively. While uracil is nearly non-fluorescent in the majority of solvents, in hydrogen bonding ones it reveals a non-vanishing quantum yield, associated to a fluorescence band that is the mirror image of the first absorption band, an indication that the absorption and emissive states are the same. The ordering of the two excited states seems therefore to be strongly influenced by specific interactions with solvent molecules. Indeed, while all the methods give rather precise predictions for the vertical energies (within +0.3 eV from the available data[105]), only the one combining a continuum model (PCM) for the bulk and 4 explicit water molecules is able to reproduce the appropriate ordering of the states and thus match the photophysical picture suggested by the experiments. This is explained by the propensity of uracil to form ordered complexes with water molecules thanks to hydrogen bonding, the inclusion of explicit solvent molecules, particularly those in the cybotactic region, is in this instance found to be a mandatory requirement to describe accurately the electronic structure and its excited state response.

The effect of solid phases on the photophysical properties of molecular systems is, on the other hand, less explored (and more complex) with respect to solution. Although implementations of TD-DFT or similar approaches exist for extended periodic systems (see refs. 106 and 107 for instance), such calculations remain however rather computationally-demanding with hybrid functionals, especially for large systems with low symmetry. A widely employed approach in the study of AIEgens is then to consider clusters where a photoactive subset of molecules, e.g., monomer or dimer, are treated with quantum chemical methods while the surrounding molecules are treated with a less demanding method that ensures nonetheless the appropriate description of short-range Coulomb interactions and polarization effects. The characteristics of the cluster depend on the morphology of the solid phase that can either be disordered for amorphous solids or ordered for crystallites in powders or polycrystalline films.

The study of amorphous systems is routinely carried out by performing large-enough molecular dynamics simulations from which a configurational sampling for small aggregates, often with the inclusion of explicit solvent molecules, are extracted. These configurations are used to perform a series of high level (QM) calculations on a photoactive unit inside the aggregate while the rest is treated at a lower level (QM´ or MM)[108-110]. In the context of SLE/AIE the most widely employed MM force fields used in QM/MM approaches are the universal force field (UFF)[108] and the generalized Amber force field (GAFF)[109,110], often refined using the results of higher-level calculations on isolated structures from which also atomic charges are obtained. While for QM/QM´ approaches the choice of the lower level

of theory largely depends on the higher QM level. It usually involves methods with a reduced computational cost combined with compact basis sets, such as Hartree-Fock with a small basis, e.g., 3-21G* [108] or STO-3G.

The modeling of crystalline morphologies instead relies on the knowledge of the specific packing arrangements present in the crystalline samples. These latter may be directly derived from experimental data or from theoretical predictions of the most stable packings and are used to define the molecular aggregates to be used for properties calculations at the QM/MM or QM/QM´ levels.

An apparent drawback of QM/MM and QM/QM´ methods is the freedom and arbitrariness in the selection of the cluster size, that is a major factor in defining both the computational load of the calculation and the quality of the results. Large clusters are naturally more demanding but are sometimes required since the effect of an increasing size on photophysical properties might be important over a non-trivial range. Indeed, it should be stressed that long range Coulomb interactions, of great importance for photophysical properties, are usually not smoothly converging with the cluster size[111]. Another issue concerns how these models compare in size with the aggregates for which experimental data are collected. Amorphous aggregates come with a distribution of sizes and their packing could express a number of local environments that have to be sufficiently sampled in order to produce reliable predictions of the aggregate responses. For those phosphors that mostly exhibit emission enhancement in ordered aggregates, an approach that improves on QM/MM (or QM/QM´) methods and that may be combined with these, is to exploit the knowledge of the periodic electronic structure of the crystal packing to produce distributions of point-like charges to be used as embedding backgrounds for the photoactive unit[112-114]. These distributions provide a good approximation to both short- and long-range Coulomb interactions and achieve particularly effective descriptions of the bulk electrostatic environment at reduced cost. In addition, in many instances these embeddings reasonably reproduce all major constraints provided by the solid phase and are able to accurately describe the behavior of the aggregated phosphors. This electrostatic embedding approach, based on the Ewald method, has been already applied to study the photophysical properties of systems including excited-state intramolecular proton transfer[114], AIE[67], and mechanochromism[115] in molecular crystals but also systems with reduced one-dimensional (1D) and two-dimensional (2D) periodicities such as photoactive CdSe (0D) quantum dots and 2D nanoplatelets[116] as well as more complex heterointerfaces[117].

As depicted in Figure 3, within this approach, a finite cluster representing the chromogenic unit, is extracted from a periodic structure and embedded in a total charge array obtained by replicating crystallographic unit cells. Point Charges (PC) are placed at the positions of the crystallographic atoms. The system is then partitioned into three zones: (i) an inner first zone (Z_1) containing the cluster to be treated explicitly at the QM level composed of N_1 atoms; (ii) an intermediate second spherical layer (Z_2) with N_2 sites ($N_2 > N_1$), represented by fixed PC as obtained from a population analysis of the periodic calculation (e.g., Mulliken or Hirshfeld) in order to avoid artificial over-polarization of the electron density in Z_1; and finally (iii) an outer zone (Z_3) with N_3 sites ($N_3 >> N_2$) containing all other sites whose

PCs are adjusted via a fitting procedure. This charge fitting procedure consists in computing the electrostatic potential of the infinite periodic lattice at all sites of Z_1 and Z_2 by employing the Ewald lattice formula and then determining the PC values in Z_3 that reproduce the calculated Ewald potential at all sites in Z_1 and Z_2. Additionally, the fitting procedure is constrained to produce a neutral charge array and a minimum total dipole moment.

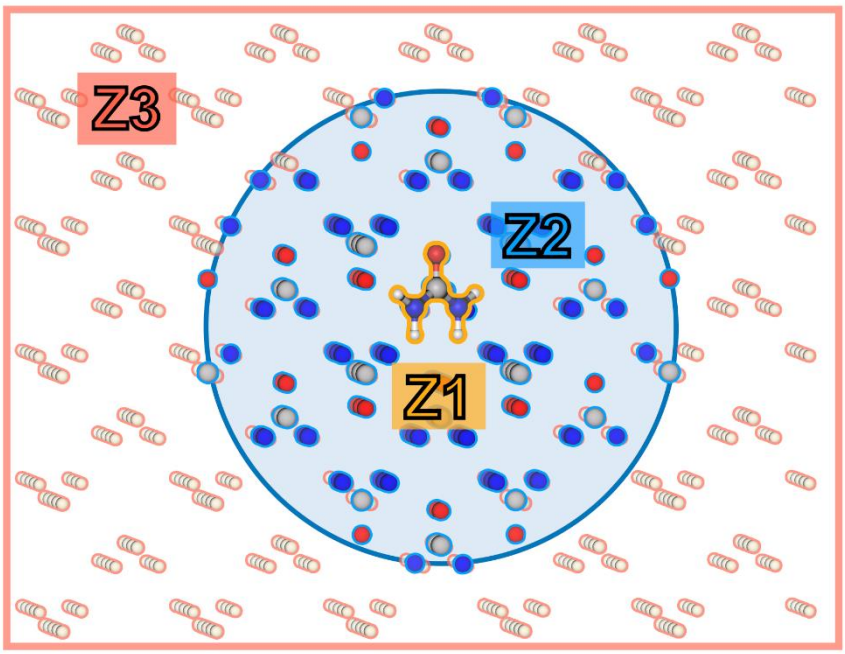

Figure 3. Schematic representation of the electrostatic embedding based on the Ewald method. The scheme highlights the three regions in which the total system, i.e., the photoactive unit and the array of point charges, is divided. For the sake of clarity only a portion of the point charges in Z3 are shown and Z2 has been shrunk. For typical organic crystals, the total number of charges is in the order of 10^5 with zone 3 being 10 to 100 times more populated than Z2.

When the modeling has higher requirements, a further improvement that is very relevant for the prediction of photoluminescence consists in approximating the reaction of the environment to the structural reorganization of the photophysical unit at the excited state. This can be done in many ways, an approximate yet interesting possibility is to adapt recursively the PC embedding distribution to the excited-state structure while it is relaxing until the minimum geometry is found. A drawback of this self-consistent approach is that the response is computed by exploiting the periodicity of the system and the local character of the rearrangement is lost, i.e., for an actual system in standard conditions, the excitation likely acts as a defect in the crystal lattice and only a few layers of molecules around it are involved in the reorganization.

Once the modeling strategy has been defined for the two environments, there are specific physical quantities that needs to be targeted together with the commonly predicted photophysical properties, i.e., transition energies and the related oscillator strengths.

Ideally, these calculated properties should lead to the evaluation of the radiative and non-radiative rates (k_r and k_{nr}). While the first can be easily obtained[118], the second often require the derivation of many parameters that are not always straightforward to estimate accurately. For this reason, in this perspective, we will look at specific quantities that are able to reveal the eventual solid-state enhancement in photoluminescence while being accessible with simple calculations.

We have already stressed how the main changes between the two environments are reflected in modifications of the PES and how impractical it usually is to derive a mapping of this surface. Quantities that may give a direct assessment of these modifications are the Huang-Rhys (HR) factors[119-121]. Despite suffering of 'nearsightedness' due to harmonic approximation underlying their derivation, HR factors offer a straightforward diagnostic tool to highlight differences of the local minima on the adiabatic surfaces involved and they also provide a measure of the coupling strength between electronic and vibrational degrees of freedom, a parameter that is of course highly relevant in the process of non-radiative decay.

HR factors have been originally introduced to estimate the non-radiative transitions following photon absorption in a lattice with F-centers[121] and have been then generalized to non-periodic and rigid molecular systems. The coupling between electronic and vibrational degrees of freedom is evaluated by assuming that the minimum of the PES maintains the same shape in the excited and in the ground state, i.e., the normal modes frequencies remain unchanged, and the two minima are simply shifted in the multi-dimensional space by some shift vector.

By comparing the minimum geometries in the two states it is possible to evaluate the shift vector and estimate how much each normal mode is involved in the geometry reorganization. Mathematically, we can write:

$$d_j = \frac{1}{m_j \Omega_j^2} \frac{\partial \mathrm{E}^{\mathrm{exc}}}{\partial q_j} \tag{2}$$

for the entry of the shift vector related to the *j*-th normal mode. Here, m_j and Ω_j are the reduced mass and the frequency of the q_j normal mode. These displacements are then used to estimate the dimensionless HR factors according to:

$$HR_j = \frac{m_j \Omega_j}{2\hbar} d_j^2 \tag{3}$$

The underlying assumptions are (i) that the molecule keeps the same number of nuclear degrees of freedom before and after reorganization and (ii) the shape of the local PES in the harmonic approximation in the ground and excited state remains more or less the same. The second assumption cannot be assumed to hold in most cases pertaining AIEgens, that in general cannot be regarded as rigid molecules and are concerned with substantial geometry reorganizations in the excited state.

Despite this, HR factors are still very informative even outside their theoretical range of validity. Often in fact, they are able to offer a good indication on whether a compound will have SLE/AIE character or

not. If nuclear and electronic degrees of freedom are strongly coupled (large HR factors), this usually indicates that the molecule undergoes a reorganization that will allow the exploration of a sizable portion of the PES. This dramatically increases the probability of encountering a CI or accessing regions where the deexcitation mediated by vibrational modes may be more efficient. When the HR factors computed in solution are found to be substantially larger than those computed for the molecule simulated in solid phase, this is a strong indication that the molecule will exhibit increased photoluminescence once aggregated.

Another important issue concerning the modeling, regards the electronic structure methods that need to be used to provide accurate predictions for the relevant quantities, such as geometries and the associated energies together with the local PES via the normal mode frequencies, i.e., second derivatives, of the structures. The accuracy and reliability of these last are heavily impacted by the description of noncovalent interactions known to be particularly difficult to model[122,123].

Among the many theoretical investigations, the ones that are more thorough often deploy multireference methods that are quite expensive from a computational point of view. The most commonly used are CASSCF, CASPT2 or their combinations[49,50,61,124] whose results are often compared to the ones of multireference configuration interaction (MRCI)[125-127].

These methods allow, among other things, the identification of CI seams in the PESs and, combined with nonadiabatic quantum dynamics simulations, offer the possibility of directly computing the deexcitation rates k_{nr} associated with these CIs. Unfortunately, due to their scaling with system size, these methods can hardly be deployed for the study of many of the typical AIEgens, that are rather large molecular systems. In this regard, DFT and its time-dependent extension (TD-DFT) remain probably unrivalled in terms of scalability and adaptability for the study of the excited state manifold, especially when the envisaged goal is to provide fast diagnostic tools for the in-silico screening of AIEgen performances in the relevant environments. Nonetheless, it has to be stressed that the description of the molecular processes involved in SLE/AIE still constitutes a formidable challenge for DFT based approaches. Indeed, in its most widely employed formulation, TD-DFT is known to provide unsatisfactory descriptions of CIs[128] that do not permit the assessment of deexcitation rates as other methods do. In addition, despite some recent improvements, most DFT approaches have less-than-ideal performances in the description of noncovalent interactions[129-131], that play a major role in the aggregation phase modulation of photoluminescence for virtually all known AIEgens. Despite these shortcomings, that have already been partially addressed via the development of derived methods able to overcome these difficulties, like spin-flip TD-DFT (SF-TD-DFT)[132,133], even standard DFT and TD-DFT offer good-enough predictions for equilibrium geometries, the associated energies and local PES topology[134-136].

Adopting a more pragmatic take, DFT predictions, although not ideal in some respects, can help achieve a modeling accuracy largely sufficient for clarifying the most salient features of the various molecular mechanisms behind SLE/AIE. Indeed, by exploiting the data on the PESs conveyed by parameters such

as the HR factors, it is possible to identify the molecular motions responsible for the access to the most important deexcitation channels in solution and how this access is restricted upon the change in aggregation phase at the cost of renouncing a full quantitative prediction of non-radiative rates and thus the assessment of the actual AIE magnitude through the comparison of simulated quantum yields in the two environments.

4. Selected case studies

The discussed quantum chemistry methods have already been deployed to study many molecular systems exhibiting SLE/AIE behavior. In the following, some examples that are particularly relevant for the present discussion are reviewed. Despite the variety of systems presented that are quite diverse in their chemical nature, see schemes in Figure 4, throughout the discussion we will attempt to bring forth and highlight the common features of the phenomenon. The first case analyzed will be that of novel material based on tetraphenylethene (TPE) to prove that the approach outlined above is indeed able to provide a sound interpretation of the standard AIE mechanism for the fluorophores belonging to the first large class of materials responsible for the revival and expansion of this research domain starting from the early 2000s[136]. Then, after demonstrating the role of conformational reorganization in non-radiative decay and its inhibition in the aggregated phase, we will move to another material for which the solid phase, more specifically the crystal, is responsible for a luminescence enhancement of the first excited state thanks to the influence of an environment that affects the features of the structural reorganization at the excited state and that strongly enhances the radiative rate by polarizing the photophysical unit. Finally, we will approach the family of compounds that display a solid-state enhancement in photoluminescence as a result of an excited-state intramolecular proton transfer.

A particular accent will be also given to how similar mechanisms might originate in rather different contexts and the additional challenges posed to the modeling in these cases.

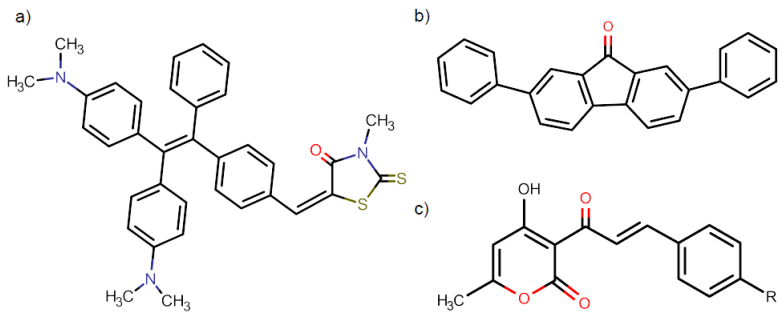

Figure 4. Schematic representation of the three molecular systems discussed in the text. In the different panels are reported the structures for : (a) TPE-MRh, a tetraphenylethene (TPE) derivative functionalized with 2 donor dimethylammine moieties and a rhodanine acceptor (from ref. 137)**;** (b) diphenylfluorenone, an AIEgen material with a weak anti-Kasha fluorescence in solution and an emission enhancement of the Kasha-like fluorescence in the crystalline phase, from ref. 67 and (c) cinnamoyl pyrone derivatives investigated in ref. 138 for their solid-state fluorescence prompted by the excited state intramolecular proton transfer (ESPT).

4.1 Restriction of motions: TPE-MRh

As previously mentioned, AIEgens with bulky functional groups and complex tridimensional geometries, often dubbed 'propeller-shape' AIEgens, have been the subject of intensive research during the last two decades[16,37,139]. Due to this interest and the rather intuitive character of the molecular mechanism behind their increased luminescence in solid state governed by the blocking of molecular motions, these systems are actually over-represented in the category of AIE fluorophores and have become widespread as functional units or motifs to induce the AIE behavior in larger systems with other desirable responses[140-142]. In the framework of our discussion, it is instructive to analyze the case of a tetraphenylethene (TPE) derivative (TPE-MRh, Figure 4(a)), functionalized with two electron donating amino groups and a rhodanine acceptor that has been the object of a combined experimental and theoretical study[137]. Among the AIE-inducing motifs cited, TPE may be plausibly considered as the prototypical AIEgen, with a fluorescence in solution that is completely quenched in non-viscous solvents but a pronounced photoluminescence in the aggregated state (amorphous mostly)[143-146]. For TPE, the mechanism for enhanced luminescence in the solid state is due to a restriction of the motions of the phenyls attached to the double bond, preventing the molecular geometry to reach regions of the PES where a CI is likely present and accessible[146,147] thus realizing a RACI scenario. Experimental data for TPE-MRh have revealed that functionalization affects the behavior of the molecule in more than one way[137]. In solution the compound displays a faint fluorescence that is substantially enhanced in solid state with more than a six-fold increase (see Figure 5).

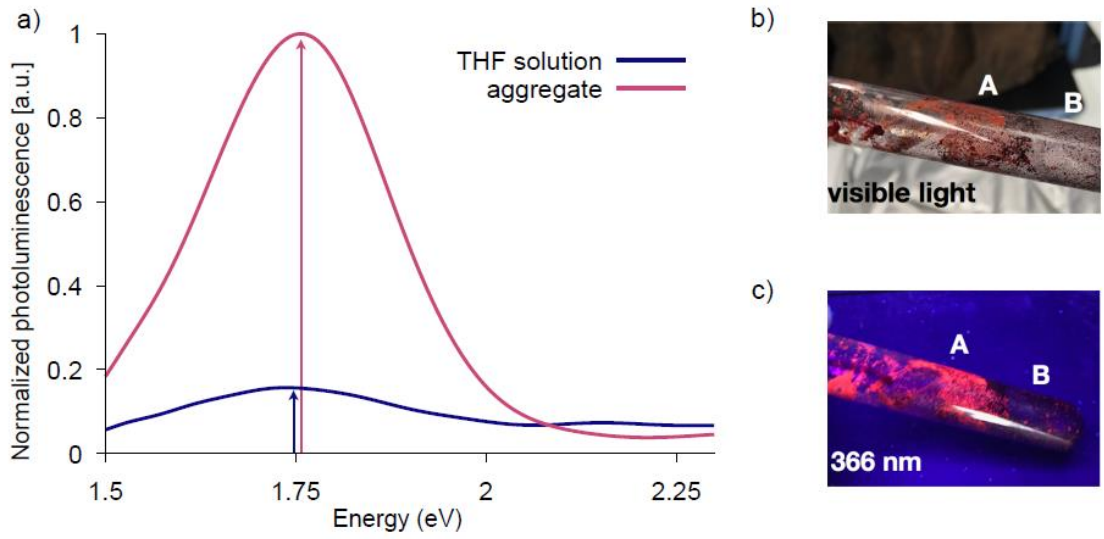

Figure 5. (a) Experimental emission of TPE-MRh in solution (blue) and in the aggregates (magenta) formed in a mixture of water (90%) and THF (10%) at the same concentration of $5 \cdot 10^{-5}$ M, after irradiation at 490 nm (2.53 eV). The photoluminescence experiences an almost 6-fold increase upon aggregation, displaying a pronounced aggregation-induced enhanced emission (AIEE) effect, data are taken from ref. 137. Panels (b) and (c) show the fluorescence of the aggregates extracted from the solution under visible light (b) and under irradiation with a UV lamp at 366 nm (3.39 eV), adapted with permission from ref. 137.

The presence of a faint fluorescence suggests that the accessibility of the eventual CI or the deexcitation mediated by molecular vibrations are decay pathways far less efficient than for TPE. This is possibly due to a structural rigidification caused by the grafting of groups with opposite electron-withdrawing and electron-donating tendencies, that is reflected in a less pronounced modification of the molecular PES in the solid phase. The addition of these groups also makes TPE-MRh bulkier than TPE. Despite the increased steric hindrance, this seems to promote stronger interactions between neighboring molecules upon aggregation that favor the formation of small ordered aggregates (crystallites) with molecular packings having a similar effect on emissive properties, i.e., a blueshift of the emission due to the anisotropic polarization and to changes in the excited state geometries. In these ordered aggregates, the formation of excimers can be ruled out since closest contact distances of the active moieties are too large.

Taking advantage of the sound understanding of the AIE molecular mechanism for TPE, a comparative analysis may be carried out exploiting the data on numerical HR factors for both molecules in solution. However simple, the observation of substantially smaller HR factors for TPE-MRh with respect to TPE, has been sufficient to explain the presence of the faint fluorescence in solution and to give a good indication of the mechanism at play. Therefore, to explain the AIE or better, the AIEE (aggregation-induced enhanced emission) character, additional analyses in the solid state have been conducted.

In particular, to approximate the solid-state environment, two different modeling approaches have been considered. The first has consisted in the derivation of a set of Ewald embedding distributions reproducing the static polarizability of the bulk environment associated to the set of polymorphs that have a high probability of being populated at experimental conditions. These packing arrangements have been predicted via Monte-Carlo sampling methods and subsequently refined via periodic-DFT calculations, according to a protocol that has already been successfully deployed for the study of other systems.

From the embedded TD-DFT calculations fluorescent deexcitation energies have been computed and found in reasonable agreement with experiments.

In addition to this strategy, a more computationally expensive analysis has been performed on the polymorph with the lowest overall energy. A supercell has been constructed containing 24 molecules from the optimized DFT unit cell. In this cluster, a central molecule has been selected to be the photoactive unit of interest and multilevel QM/QM´ ONIOM calculations have been performed to model the molecular reorganization experienced in the solid state (see Supporting Information for detailed computational details). The minima for the ground and the emissive state (S_1) and the frequencies of the corresponding normal modes have been obtained by keeping all the other molecules in the cluster frozen. These data have been used to calculate the HR factors which have been compared to the factors obtained from PCM solvent calculations, as depicted in Figure 6 where all the factors relative to normal modes below 500 cm^{-1} are reported. This range covers all those molecule-wide modes that are usually the most implicated in non-radiative decay. From the plot it is clear that the crystalline modes are substantially

less coupled to electronic degree of freedom due to an overall conformational reorganization that is much more constrained. Low modes in the solid have larger frequencies, indicating a 'steeper' local PES and similar structural motions in the range have HR factors that are between 150 to 200 times smaller. These numbers clearly prove the constraining effect of the crystalline packing and largely explain the reported emissive gain upon aggregation, perfectly fitting a scenario of type (i) where the k_{nr} is strongly lowered.

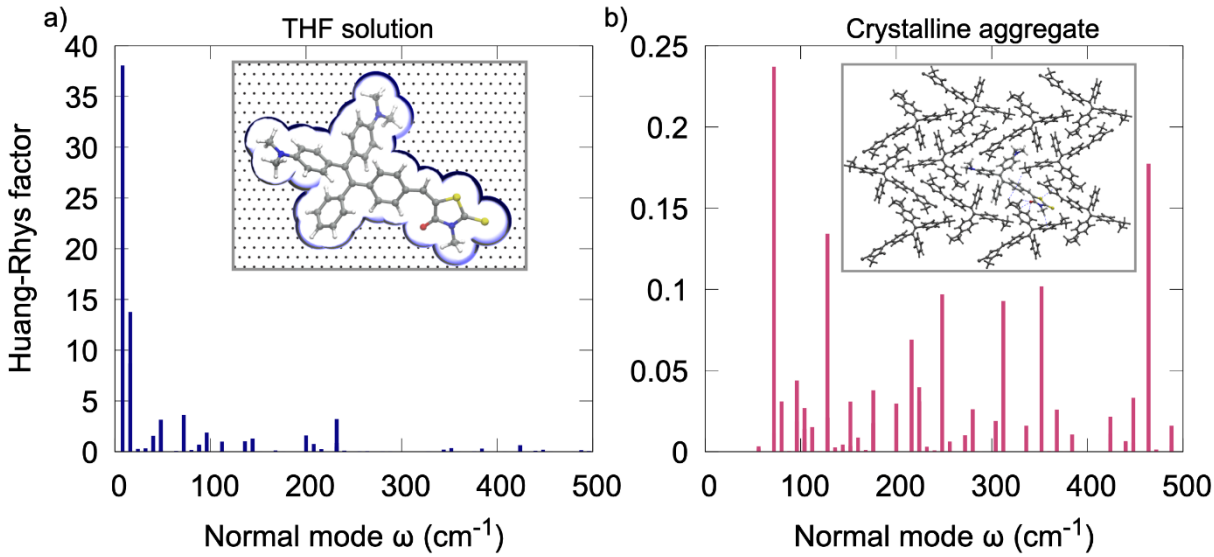

Figure 6. Comparison of Huang-Rhys (HR) factors computed in solution and solid. In panel (a), the factors are obtained from the analysis of structures at the ground and excited state simulated at DFT and TD-DFT levels with a polarizable continuum model (PCM) of THF, data from ref. 137. Panel (b) reports the factors obtained from the comparison of the ground and excited state structure of a TPE-MRh fluorophore. The relaxed structures in this case are obtained by simulating the molecule embedded in a cluster of 23 molecules built according to the packing found in the most stable crystalline structure using a QM/QM' multi-level approach according to the ONIOM scheme (see Supporting Information for computational details). A clear restriction of the reorganization upon excitation due to the crystalline environment can be inferred from the comparison of the two sets of HR factors reported in panel (a) and (b).

4.2 Modulation of the radiative decay due to the environment

Another interesting compound that has been reported[148-150] to have SLE/AIE character is 2,7-diphenylfluorene (DPF), see Figure 4(b). The photoluminescence of DPF is quite remarkable as it involves two distinct and well separated bands, one at higher energy with a bright peak at 3.8 eV and another at 2.3 eV. The redshift and the broadened character of the low-energy peak has suggested that its origin is linked to the formation of molecular aggregates in which new photoactive species emerge resulting from the formation of an excimer. To test this hypothesis, in a recent study[66] some of the authors have investigated the emissive properties in solution and in the solid state by using both a hybrid QM/QM´ ONIOM and a periodic Ewald embedding approach. Following the scheme suggested above, the comparison between calculations in the solvent (THF) using the implicit C-PCM solvent model and in solid state has allowed to sketch the molecular mechanism. This is interpreted as a single-molecule

emissive phenomenon where the luminescence enhancement comes from the anisotropic polarization of the local crystalline environment that constrains the conformational reorganization at the excited state (S_1) and affects the character of the transition.

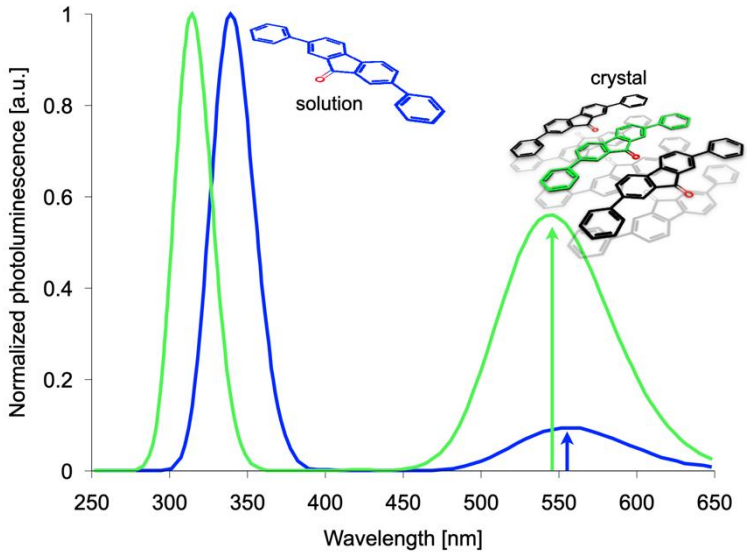

Figure 7. Simulated emission spectra of both $S_1 \rightarrow S_0$ and $S_3 \rightarrow S_0$ transitions at the TD-CAM-B3LYP level: i) in THF implicit solvation, C-PCM, blue solid line and, ii) in the solid state, green solid line, via the SC-Ewald embedding procedure detailed in the text. Data taken from ref. 66.

Indeed, as shown in Figure 7, the calculations performed clearly suggest that the high-energy peak is associated with the deexcitation from S_3 to S_0, hence indicating an anti-Kasha behavior for DPF in solution, that is also compatible with the very small quantum yield in this medium. The low-energy emissive band (attributed to the deexcitation from S_1 and computed to be of charge transfer type) experiences a strong enhancement when going to the crystalline phase. In order to reveal and explain the AIE character, the solid state has been modelled via a point-charge embedding distribution derived, as previously described, from the optimized structure of the main polymorph unit cell[66]. In this case, the distribution obtained initially has been allowed to relax along with the optically active unit, consisting of a single molecule excited at S_1. This procedure, called self-consistent Ewald (SC-Ewald) embedding[114], implements the recursive modification of embedding charges along the relaxation path of the active on the excited state PES. Upon convergence of both structure and distribution, the final combination provides an approximate description of the medium response both in terms of the geometrical changes of the structure and the mutual polarization between the active unit and its local environment. For DPF, the final structure reveals an almost four-fold increase in emissive strength for the S_1 to S_0 transition compared to solution, directly signaled by an increase of the oscillator strength. This can be interpreted as the effect of the anisotropic polarization of the whole crystalline medium emerging as a response to the local excitation of the active unit at S_1. These results indicate, for DPF, a scenario of type (ii) where the luminescence enhancement in the solid state is caused by an increase of

the radiative rate rather than a decrease of the non-radiative one. Clearly though, this effect originates from the different structural reorganization imposed by the medium constraints simulated with the SC-Ewald procedure with an additional effect of the final polarization.

The peculiarity of the mechanism identified suggests that in this case the response of the environment is fundamental in modulating the structural modifications and the changes in medium polarizability that determine the excited state dynamics.

4.3 Excited state intramolecular proton transfer

Alongside 'propeller-shape' structures, another large class of molecules often included in the AIE family is the one that groups compounds undergoing excited-state intramolecular proton transfer (ESIPT)[151-153]. Although this categorization is debated[24], as the emissive species changes from the one in absorption and the SLE label would thus be better fitting, from a macroscopic point of view the phenomenology is indistinguishable from those of other AIEgens. In the case of ESIPT materials, the different structures in absorption and emission attenuate resonant energy transfer phenomena in the solid, thus largely preventing ACQ. The number of compounds investigated within this class is remarkable (see ref. 154 and references therein), the studies on their behavior are usually carried out on sets of systems derived from the same selected skeleton and their properties are compared. While the ESIPT mechanism is usually maintained throughout the set, the substituted groups are implicated in the modulation of the interaction with the environment, both in solution and in solid. These comparative analyses offer precious insight into the range of behaviors depending on the packings that are determined by the steric constraints of the substituents. The general mechanistic picture for ESIPT compounds, identifies a common series of steps governing the structural response of the system. Upon photon absorption the proton transfer at the excited state is favored. Once the proton has been transferred, the excited trans isomer of the keto form is the species potentially responsible for the emission. However, the radiative decay is in competition with the photoinduced isomerization from trans to cis form. The ability to undergo the extensive conformational change implied by the isomerization, largely depends on the constraints put in place by the local environment. If it is allowed, the system explores a large portion of the PES and this often results, depending on the specific system, in encountering a CI seam or reaching regions where vibrational deexcitation is more efficient. Indeed, the RACI mechanism is often called upon to explain the vanishing or faint emission of many ESIPT molecules in solution[62].

Recently, one of these comparative studies has been carried out on a molecular set derivatized from a cinnamoyl pyrone (CP) skeleton[138], see Figure 4(c). Substituents were chosen among groups with either electron withdrawing or donating character. All studied compounds have been shown to undergo ESIPT with the majority transitioning from being non or very faintly fluorescent in solution to moderately fluorescent in crystalline phase, where photoluminescence quantum yields have been reported between 0.04 and 0.32. For a subset of these compounds including the unsubstituted CP and a derivative carrying a dimethylamine moiety, a thorough theoretical analysis has been able to provide a specific picture of

the general mechanism sketched above. In this case, due to the complexity of the steps, the sole analysis of the local shape of the PES (via the HR factors) for the fluorescent species, i.e., trans isomer of ketonic form, would not provide enough information. For this reason, a mapping of the PES region explored by the reorganization has been realized thanks to SF-TD-DFT methods. The calculations, carried out in vacuum and in solvent, have been able to confirm the involvement of a CI seam that is reached during the rotation of the pyrone moiety (see Figure 1 and Figure 8), the configurational change leading to the isomerization. This conformational change is plausibly prohibited or strongly inhibited in the solid, where the packing likely makes the energetic cost very high.

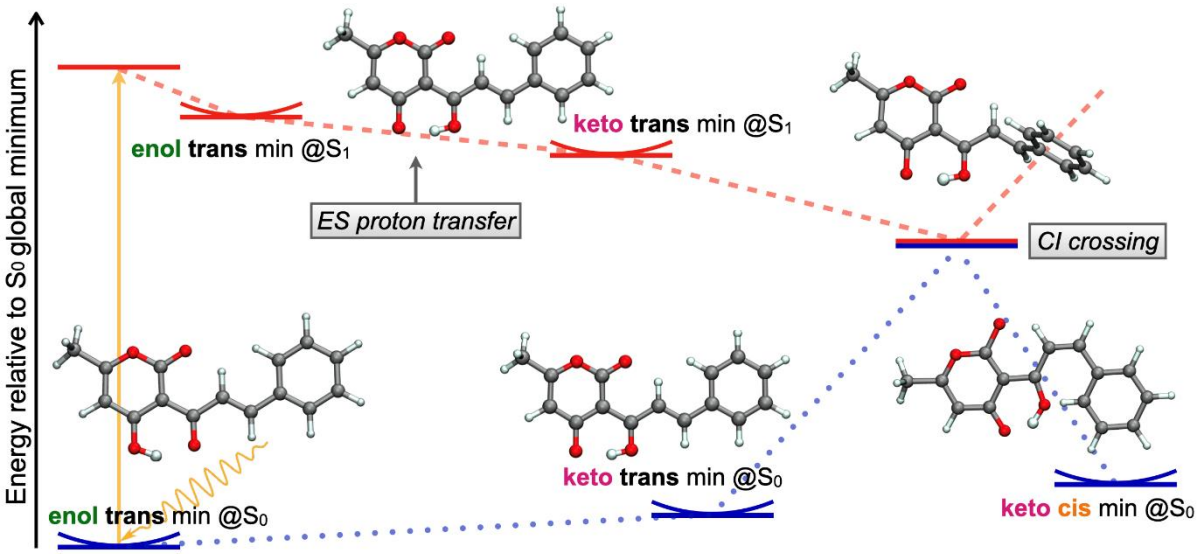

Figure 8. Sketch of the potential energy profile reorganization pathway undergone by cinnamoyl pyrone upon excitation to S_1, as obtained from the SF-TD-DFT simulation of the system reported in ref. 138. After excitation to the first excited state (S_1) from the enolic most stable ground state form (enol trans), the system relaxes to the S_1 enol minimum where the planarized geometry and altered bond lengths promote the proton transfer and the formation of the keto form. Once the proton transfer has taken place the molecule relaxes to the minimum of the trans keto form (keto trans), that is understood to be the main emissive species in solid state. If the molecule is not constrained by the environment, it undergoes a trans-to-cis tautomerization during which a CI is encountered. Through the CI the system transitions non-radiatively to the ground state. The energy reference is taken to be the trans enol form global minimum on S_0.

The heavy calculations needed to carry out this analysis in solid though, have not been performed. The analysis also points out that the substituents are able to modulate the topology of the access to the CI seam, e.g., peaked or sloped, thus impacting the balance between radiative and non-radiative rates. A balance that is further affected by the rigidification caused by aggregation in favor of radiative channels, thus realizing also in this case a RACI scenario of type (i). The authors also point out that many of the solid-state luminescence decay curves carry, for the molecules in the set, 'multiple exponential character' suggesting the involvement of excited states with different characteristics and weights determined and modulated by multiple solid-state environments for each system. ESIPT compounds appear therefore to express a molecular mechanism that is somewhat peculiar with respect to other AIEgens but that can be

ultimately traced back to a transition from a rigid ground state to a more flexible excited state structure prone to large conformational changes that are once again hindered or expressed depending on the environment.

5. Conclusions

The cases detailed offer the chance to outline a few general features of the molecular mechanisms underlying the complex macroscopic phenomenon of solid-state enhanced luminescence. The systems described display quite varied molecular structures, but a few patterns emerge suggesting a possible common rationale, that may be generalized over a number of compound classes showing SLE/AIE. For a start, it is usually possible to distinguish a core that is preeminently involved in light absorption bonded to one or more aromatic moieties. The link between the core and the peripheral moieties is typically a single bond and, upon photoexcitation, a redistribution of the electronic density from the core towards the outer groups causes a destabilization of the ground state geometry in terms of bonding pattern and a loss of rigidity. This flexibility enables the structure to experience potentially pronounced conformational changes upon relaxation whose expression crucially depends on the constraints -usually steric- imposed by the local environment that, if allowed, promote the non-radiative loss of energy via RIM or RACI mechanisms. Propeller-shape AIE fluorophores are probably the most straightforward example of this class and hold, as already stressed, the merit of ensuring a high degree of transferability of the SLE behavior. Indeed, whenever they are integrated in larger architectures or are functionalized with groups to elicit additional responses, the behavior appears to be consistently displayed. These compounds therefore constitute probably the most convenient choice to introduce AIE responses in novel functional materials. ESIPT compounds, despite the more convoluted mechanism, can be said to undergo a similar process when the bond structure reorganization following the photo-induced proton transfer triggers, also in this case, a conformational change, i.e., the trans-cis isomerization, whose realization depends, again, on the energetic cost determined by the molecular environment.

This general picture also offers insights on the minimal and maximal size for a molecule to exhibit an SLE/AIE behavior. The maximal size appears to be constrained on one side by the length-scale of electronic density redistribution upon photon absorption across the core and the peripheral groups. On the other side, another constraint is the fact that the conformational changes involving these last, should be ‘fast enough’ to happen within the typical time-scales of radiative decay in order to compete with fluorescence. A requirement for the minimal size comes instead from the character of the molecular packing that is once again determined by the interactions of the peripheral groups. This packing should not be excessively tight because this might lead to radiative losses due to energy transfer processes. Clearly, this holds true unless the material exhibits enhanced luminescence because of excimer formation or due to ESIPT. Indeed, compounds belonging to this last group often have smaller structures since the difference in the absorbing and emissive species already inhibits transfer processes.

These observations also suggest that the classes of compounds displaying SLE/AIE are likely more numerous than what is currently recognized and that a 'similarity' bias in the exploration of the chemical space, especially for propeller-like structures, is likely to blame for this. The general idea that emerges offers a recipe for a more rational search and design of AIE fluorophores. In summary, the requirements that need to be met include the simultaneous presence of a core with a photophysical response of interest for a specific application, e.g., a particular emission wavelength, and peripheral moieties linked to it able to affect its electronic structure in a substantial way via conformational changes that are allowed in diluted phase and that promote deexcitation. This intramolecular interaction should go together with intermolecular ones giving low-energy molecular packings for which, the same conformational changes of the peripheral groups are severely restrained.

This understanding clearly prospects the possibility of devising protocols for the computationally assisted design of new SLE/AIE materials. The greatest hurdle to successfully achieve this remains the development of 'simple' and straightforward descriptors able to provide a prediction of the balance between these intramolecular and intermolecular interactions that results from the choice of specific core and peripheral pairings. HR factors appear as good candidates to fulfill this role, but others should be developed to better signal the changes in electronic density characterizing the mechanism.

Understanding the complex interactions between molecular units and their environment remains currently one of the most important challenges of modern quantum chemistry. Acquiring descriptive and predictive power over these interactions prospects possibilities that go well beyond the design of luminescent materials in pure aggregates. Indeed, knowledge and control of the forces at play directly translates into the ability to elicit enhanced luminescence in very specific and different environments. For example, SLE responses could be engineered for ordered aggregates of two or more compounds, i.e., co-crystals[155], or fluorophores dispersed in polymer matrices as composites or blends, thus exponentially increasing the versatility and specificity of the functional materials derived, resulting in an increased ability to respond to specific requirements that are needed to enhance and further many important technological fields.

Supporting Information

Computational details concerning the calculation of HR factors in condensed phase for the TPE-MRh system.

Acknowledgements

The authors would like to warmly acknowledge Prof Andrea Pucci (UniPisa, Italy), Dr Francesco Muniz-Miranda (UniMore, Italy), Dr Cristina Gellini (University of Florence, Italy) and Dr Davide Presti (Paris) for fruitful discussions. GENCI is gratefully acknowledge for granting access to HPC resources under different allocations of project A0050810135. Qinfan Wang is funded by the China Scholarship Council (n. 202006890004).

References

1) V. Podzorov, Building molecules for a function, *Nat. Mater.*, 2010, **9**, 616–617.
2) R. L. Carroll and C. B. Gorman, The Genesis of Molecular Electronics, *Angew. Chem. Int. Ed.*, 2002, **41**, 4378–4400.
3) O. Ostroverkhova, Organic Optoelectronic Materials: Mechanisms and Applications, *Chem. Rev.*, 2016, **116**, 13279–13412.
4) T. Itoh, Fluorescence and Phosphorescence from Higher Excited States of Organic Molecules, *Chem. Rev.*, 2012, **112**, 4541–4568.
5) Z. Yang, Z. Mao, Z. Xie, Y. Zhang, S. Liu, J. Zhao, J. Xu, Z. Chi and M. P. Aldred, Recent advances in organic thermally activated delayed fluorescence materials, *Chem. Soc. Rev.*, 2017, **46**, 915–1016.
6) H. Nakanotani, Y. Tsuchiya and C. Adachi, Thermally-activated Delayed Fluorescence for Light-emitting Devices, *Chem. Lett.*, 2021, **50**, 938–948.
7) D. Jacquemin, E. Brémond, A. Planchat, I. Ciofini and C. Adamo, TD-DFT Vibronic Couplings in Anthraquinones: From Basis Set and Functional Benchmarks to Applications for Industrial Dyes, *J. Chem. Theory Comput.*, 2011, **7**, 1882–1892.
8) P. S. Hariharan, N. S. Venkataramanan, D. Moon and S. P. Anthony, Self-Reversible Mechanochromism and Thermochromism of a Triphenylamine-Based Molecule: Tunable Fluorescence and Nanofabrication Studies, *J. Phys. Chem. C*, 2015, **119**, 9460–9469.
9) M. Shimizu and T. Hiyama, Organic Fluorophores Exhibiting Highly Efficient Photoluminescence in the Solid State, *Chem. - Asian J.*, 2010, **5**, 1516–1531.
10) M. Van der Auweraer, Z. R. Grabowski and W. Rettig, Molecular structure and the temperature-dependent radiative rates in Twisted Intramolecular Charge-Transfer and exciplex systems, *J. Phys. Chem.*, 1991, **95**, 2083–2092.
11) J. Ferguson and A. Mau, Spontaneous and stimulated emission from dyes. Spectroscopy of the neutral molecules of acridine orange, proflavine, and rhodamine B, *Aust. J. Chem.*, 1973, **26**, 1617.
12) N. Benson, O. Suleiman, S. O. Odoh and Z. R. Woydziak, Pyrazole, Imidazole, and Isoindolone Dipyrrinone Analogues: pH-Dependent Fluorophores That Red-Shift Emission Frequencies in a Basic Solution, *J. Org. Chem.*, 2019, **84**, 11856–11862.
13) J. Han and K. Burgess, Fluorescent Indicators for Intracellular pH, *Chem. Rev.*, 2010, **110**, 2709–2728.
14) T. D. James, K. R. A. Samankumara Sandanayake and S. Shinkai, Chiral discrimination of monosaccharides using a fluorescent molecular sensor, *Nature*, 1995, **374**, 345–347.
15) J.-P. Desvergne, F. Fages, H. Bouas-Laurent and P. Marsau, Tunable photoresponsive supramolecular systems, *Pure Appl. Chem.*, 1992, **64**, 1231–1238.
16) K. Kokado and K. Sada, Consideration of Molecular Structure in the Excited State to Design New Luminogens with Aggregation-Induced Emission, *Angew. Chem.*, 2019, **131**, 8724–8731.
17) T. Förster, Energy migration and fluorescence, *J. Biomed. Opt.*, 2012, **17**, 011002.
18) J. S. Lindsey, M. Taniguchi, D. F. Bocian and D. Holten, The fluorescence quantum yield parameter in Förster resonance energy transfer (FRET)—Meaning, misperception, and molecular design, *Chem. Phys. Rev.*, 2021, **2**, 011302.
19) D. L. Dexter, A Theory of Sensitized Luminescence in Solids, *J. Chem. Phys.*, 1953, **21**, 836–850.
20) J. B. Birks, *Photophysics of aromatic molecules*, Wiley-Interscience, London, 1970.
21) E. E. Jelley, Spectral Absorption and Fluorescence of Dyes in the Molecular State, *Nature*, 1936, **138**, 1009–1010.
22) G. Scheibe, Über die Veränderlichkeit der Absorptionsspektren in Lösungen und die Nebenvalenzen als ihre Ursache, *Angew. Chem.*, 1937, **50**, 212–219.

23) Y. Hong, J. W. Y. Lam and B. Z. Tang, Aggregation-induced emission: phenomenon, mechanism and applications, *Chem. Commun.*, 2009, 4332.
24) J. Gierschner, J. Shi, B. Milián-Medina, D. Roca-Sanjuán, S. Varghese and S. Park, Luminescence in Crystalline Organic Materials: From Molecules to Molecular Solids, *Adv. Opt. Mater.*, 2021, **9**, 2002251.
25) J. Mei, N. L. C. Leung, R. T. K. Kwok, J. W. Y. Lam and B. Z. Tang, Aggregation-Induced Emission: Together We Shine, United We Soar!, *Chem. Rev.*, 2015, **115**, 11718–11940.
26) J. Gierschner, L. Lüer, B. Milián-Medina, D. Oelkrug and H.-J. Egelhaaf, Highly Emissive H-Aggregates or Aggregation-Induced Emission Quenching? The Photophysics of All-Trans *para* -Distyrylbenzene, *J. Phys. Chem. Lett.*, 2013, **4**, 2686–2697.
27) J. Gierschner, J. Cornil and H.-J. Egelhaaf, Optical Bandgaps of π-Conjugated Organic Materials at the Polymer Limit: Experiment and Theory, *Adv. Mater.*, 2007, **19**, 173–191.
28) T. B. Hansen and H. Qu, Formation of Piroxicam Polymorphism in Solution Crystallization: Effect and Interplay of Operation Parameters, *Cryst. Growth Des.*, 2015, **15**, 4694–4700.
29) S. (Sally) L. Price, Computed Crystal Energy Landscapes for Understanding and Predicting Organic Crystal Structures and Polymorphism, *Acc. Chem. Res.*, 2009, **42**, 117–126.
30) G. R. Desiraju, Crystal Engineering: From Molecule to Crystal, *J. Am. Chem. Soc.*, 2013, **135**, 9952–9967.
31) J. Bernstein, *Polymorphism in molecular crystals*, Clarendon Press Oxford university press, Oxford New York, 2002.
32) Y. Shigemitsu, T. Mutai, H. Houjou and K. Araki, Excited-State Intramolecular Proton Transfer (ESIPT) Emission of Hydroxyphenylimidazopyridine: Computational Study on Enhanced and Polymorph-Dependent Luminescence in the Solid State, *J. Phys. Chem. A*, 2012, **116**, 12041–12048.
33) T. Mutai, H. Shono, Y. Shigemitsu and K. Araki, Three-color polymorph-dependent luminescence: crystallographic analysis and theoretical study on excited-state intramolecular proton transfer (ESIPT) luminescence of cyano-substituted imidazo[1,2-a]pyridine, *CrystEngComm*, 2014, **16**, 3890–3895.
34) K. Wang, H. Zhang, S. Chen, G. Yang, J. Zhang, W. Tian, Z. Su and Y. Wang, Organic Polymorphs: One-Compound-Based Crystals with Molecular-Conformation- and Packing-Dependent Luminescent Properties, *Adv. Mater.*, 2014, **26**, 6168–6173.
35) A. Pucci, Mechanochromic Fluorescent Polymers with Aggregation-Induced Emission Features, *Sensors*, 2019, **19**, 4969.
36) N. Guidugli, R. Mori, F. Bellina, B. Z. Tang and A. Pucci, in *Principles and Applications of Aggregation-Induced Emission*, eds. Y. Tang and B. Z. Tang, Springer International Publishing, Cham, 2019, pp. 335–349.
37) D. D. La, S. V. Bhosale, L. A. Jones and S. V. Bhosale, Tetraphenylethylene-Based AIE-Active Probes for Sensing Applications, *ACS Appl. Mater. Interfaces*, 2018, **10**, 12189–12216.
38) M. Koenig, B. Storti, R. Bizzarri, D. M. Guldi, G. Brancato and G. Bottari, A fluorescent molecular rotor showing vapochromism, aggregation-induced emission, and environmental sensing in living cells, *J. Mater. Chem. C*, 2016, **4**, 3018–3027.
39) S. Cao, J. Shao, H. Wu, S. Song, M. T. De Martino, I. A. B. Pijpers, H. Friedrich, L. K. E. A. Abdelmohsen, D. S. Williams and J. C. M. van Hest, Photoactivated nanomotors via aggregation induced emission for enhanced phototherapy, *Nat. Commun.*, 2021, **12**, 2077.
40) G. Iasilli, M. Scatto and A. Pucci, Vapochromic polyketone films based on aggregation-induced enhanced emission, *Polym Adv Technol*, 2019, **30**, 1160–1164.
41) S. Suzuki, S. Sasaki, A. S. Sairi, R. Iwai, B. Z. Tang and G. Konishi, Principles of Aggregation-Induced Emission: Design of Deactivation Pathways for Advanced AIEgens and Applications, *Angew. Chem. Int. Ed.*, 2020, **59**, 9856–9867.
42) Y. Hong, Aggregation-induced emission—fluorophores and applications, *Methods Appl. Fluoresc.*,

2016, **4**, 022003.
43) T. Simon, M. Shellaiah, V. Srinivasadesikan, C.-C. Lin, F.-H. Ko, K. W. Sun and M.-C. Lin, A simple pyrene based AIEE active schiff base probe for selective naked eye and fluorescence off–on detection of trivalent cations with live cell application, *Sens. Actuators B Chem.*, 2016, **231**, 18–29.
44) A. Accetta, R. Corradini and R. Marchelli, in *Luminescence Applied in Sensor Science*, eds. L. Prodi, M. Montalti and N. Zaccheroni, Springer Berlin Heidelberg, Berlin, Heidelberg, 2010, vol. 300, pp. 175–216.
45) Z. Zhao, J. W. Y. Lam and B. Z. Tang, Tetraphenylethene: A versatile AIE building block for the construction of efficient luminescent materials for organic light-emitting diodes, *J. Mater. Chem.*, 2012, **22**, 23726–23740.
46) Z. Shuai and Q. Peng, Excited states structure and processes: Understanding organic light-emitting diodes at the molecular level, *Phys. Rep.*, 2014, **537**, 123–156.
47) A. Pucci, Luminescent Solar Concentrators Based on Aggregation Induced Emission, *Isr. J. Chem.*, 2018, **58**, 837–844.
48) J. L. Banal, B. Zhang, D. J. Jones, K. P. Ghiggino and W. W. H. Wong, Emissive Molecular Aggregates and Energy Migration in Luminescent Solar Concentrators, *Acc. Chem. Res.*, 2017, **50**, 49–57.
49) R. Crespo-Otero and L. Blancafort, in *Handbook of Aggregation-Induced Emission*, eds. Y. Tang and B. Z. Tang, Wiley, 1st edn., 2022, pp. 411–454.
50) X.-L. Peng, S. Ruiz-Barragan, Z.-S. Li, Q.-S. Li and L. Blancafort, Restricted access to a conical intersection to explain aggregation induced emission in dimethyl tetraphenylsilole, *J. Mater. Chem. C*, 2016, **4**, 2802–2810.
51) X. Cheng, K. Wang, S. Huang, H. Zhang, H. Zhang and Y. Wang Organic Crystals with Near-Infrared Amplified Spontaneous Emissions Based on 2′-Hydroxychalcone Derivatives: Subtle Structure Modification but Great Property Change, *Angew. Chem. Int. Ed.*, 2015, **54**, 8369–8373.
52) D. Oelkrug, A. Tompert, H.-J. Egelhaaf, M. Hanack, E. Steinhuber, M. Hohloch, H. Meier and U. Stalmach, Towards highly luminescent phenylene vinylene films, *Synth. Met.*, 1996, **83**, 231–237.
53) D. Oelkrug, A. Tompert, J. Gierschner, H.-J. Egelhaaf, M. Hanack, M. Hohloch and E. Steinhuber, Tuning of Fluorescence in Films and Nanoparticles of Oligophenylenevinylenes, *J. Phys. Chem. B*, 1998, **102**, 1902–1907.
54) S. Yokoyama and N. Nishiwaki, Fluorescence Behavior of Bis(cyanostyryl)pyrrole Derivatives Depending on the Substituent Position of Cyano Groups in Solution and in Solid State, *J. Org. Chem.*, 2019, **84**, 1192–1200.
55) G.-F. Zhang, Z.-Q. Chen, M. P. Aldred, Z. Hu, T. Chen, Z. Huang, X. Meng and M.-Q. Zhu, Direct validation of the restriction of intramolecular rotation hypothesis via the synthesis of novel ortho-methyl substituted tetraphenylethenes and their application in cell imaging, *Chem Commun*, 2014, **50**, 12058–12060.
56) G. Iasilli, A. Battisti, F. Tantussi, F. Fuso, M. Allegrini, G. Ruggeri and A. Pucci, Aggregation-induced emission of tetraphenylethylene in styrene-based polymers, *Macromol. Chem. Phys.*, 2014, **215**, 499–506.
57) T. Han, L. Liu, D. Wang, J. Yang and B. Z. Tang, Mechanochromic Fluorescent Polymers Enabled by AIE Processes, *Macromol. Rapid Commun.*, 2021, **42**, 2000311.
58) M. Han, Y. Takeoka and T. Seki, Facile morphological control of fluorescent nano/microstructures via self-assembly and phase separation of trigonal azobenzenes showing aggregation-induced emission enhancement in polymer matrices, *J. Mater. Chem. C*, 2015, **3**, 4093–4098.
59) B. Meng, Y. Zhang and P. Ma, Composites with AIEgens for Temperature Sensing and Strain Measurement, *Macromol. Chem. Phys.*, 2020, **221**, 1900552.
60) L. Thieulloy, L. Le Bras, B. Zumer, J. Sanz García, C. Lemarchand, N. Pineau, C. Adamo and A.

Perrier, Aggregation-Induced Emission: A Challenge for Computational Chemistry Taking TPA-BMO as an Example, *ChemPhysChem*, 2021, **22**, 1802–1816.
61) M. Dommett, M. Rivera and R. Crespo-Otero, How Inter- and Intramolecular Processes Dictate Aggregation-Induced Emission in Crystals Undergoing Excited-State Proton Transfer, *J. Phys. Chem. Lett.*, 2017, **8**, 6148–6153.
62) L. Stojanović and R. Crespo-Otero, Understanding Aggregation Induced Emission in a Propeller-Shaped Blue Emitter, *ChemPhotoChem*, 2019, **3**, 907–915.
63) M. Kasha, Characterization of electronic transitions in complex molecules, *Discuss. Faraday Soc.*, 1950, **9**, 14.
64) A. C. B. Rodrigues and J. S. Seixas de Melo, Aggregation-Induced Emission: From Small Molecules to Polymers—Historical Background, Mechanisms and Photophysics, *Top. Curr. Chem.*, 2021, **379**, 15.
65) N. L. C. Leung, N. Xie, W. Yuan, Y. Liu, Q. Wu, Q. Peng, Q. Miao, J. W. Y. Lam and B. Z. Tang, Restriction of Intramolecular Motions: The General Mechanism behind Aggregation-Induced Emission, *Chem. - Eur. J.*, 2014, **20**, 15349–15353.
66) D. Presti, L. Wilbraham, C. Targa, F. Labat, A. Pedone, M. C. Menziani, I. Ciofini and C. Adamo, Understanding Aggregation-Induced Emission in Molecular Crystals: Insights from Theory, *J. Phys. Chem. C*, 2017, **121**, 5747–5752.
67) N. Yamamoto, Mechanisms of Aggregation-Induced Emission and Photo/Thermal *E* / *Z* Isomerization of a Cyanostilbene Derivative: Theoretical Insights, *J. Phys. Chem. C*, 2018, **122**, 12434–12440.
68) R. Iwai, S. Suzuki, S. Sasaki, A. S. Sairi, K. Igawa, T. Suenobu, K. Morokuma and G. Konishi, Bridged Stilbenes: AIEgens Designed via a Simple Strategy to Control the Non-radiative Decay Pathway, *Angew. Chem. Int. Ed.*, 2020, **59**, 10566–10573.
69) Q. Peng and Z. Shuai, Molecular mechanism of aggregation-induced emission, *Aggregate*, , DOI:10.1002/agt2.91.
70) Q. Peng, D. Fan, R. Duan, Y. Yi, Y. Niu, D. Wang and Z. Shuai, Theoretical Study of Conversion and Decay Processes of Excited Triplet and Singlet States in a Thermally Activated Delayed Fluorescence Molecule, *J. Phys. Chem. C*, 2017, **121**, 13448–13456.
71) F. J. Hernández and R. Crespo-Otero, Modeling Excited States of Molecular Organic Aggregates for Optoelectronics, *Annu. Rev. Phys. Chem.*, 2023, **74**, 547–571.
72) T. Kitamura, Y. Takahashi, T. Yamanaka and K. Uchida, Luminescence associated with the molecular aggregation of hydrocarbons doped in amorphous silica glasses, *J. Lumin.*, 1991, **48–49**, 373–376.
73) F. M. Winnik, Photophysics of preassociated pyrenes in aqueous polymer solutions and in other organized media, *Chem. Rev.*, 1993, **93**, 587–614.
74) D. Möbius, Scheibe Aggregates, *Adv. Mater.*, 1995, **7**, 437–444.
75) F. C. Spano, Excitons in Conjugated Oligomer Aggregates, Films, and Crystals, *Annu. Rev. Phys. Chem.*, 2006, **57**, 217–243.
76) J. Gierschner, Y.-S. Huang, B. Van Averbeke, J. Cornil, R. H. Friend and D. Beljonne, Excitonic versus electronic couplings in molecular assemblies: The importance of non-nearest neighbor interactions, *J. Chem. Phys.*, 2009, **130**, 044105.
77) J. Gierschner and S. Y. Park, Luminescent distyrylbenzenes: tailoring molecular structure and crystalline morphology, *J. Mater. Chem. C*, 2013, **1**, 5818–5832.
78) Y. Liu, X. Tao, F. Wang, J. Shi, J. Sun, W. Yu, Y. Ren, D. Zou and M. Jiang, Intermolecular Hydrogen Bonds Induce Highly Emissive Excimers: Enhancement of Solid-State Luminescence, *J. Phys. Chem. C*, 2007, **111**, 6544–6549.
79) T. Schillmöller, R. Herbst-Irmer and D. Stalke, Insights into Excimer Formation Factors from Detailed Structural and Photophysical Studies in the Solid-State, *Adv. Opt. Mater.*, 2021, **9**, 2001814.

80) Y. Vonhausen, A. Lohr, M. Stolte and F. Würthner, Two-step anti-cooperative self-assembly process into defined π-stacked dye oligomers: insights into aggregation-induced enhanced emission, *Chem. Sci.*, 2021, **12**, 12302–12314.
81) S. Hattori, T. Nakano, N. Kobayashi, Y. Konno, E. Nishibori, T. Galica and K. Shinozaki, Luminescence color change of [3,4-difluoro-2,6-bis(5-methyl-2-pyridyl)phenyl-κ^3N,C^1,N'] cyanidoplatinum(II) by aggregation, *Dalton Trans.*, 2022, **51**, 15830–15841.
82) F. Würthner, T. E. Kaiser and C. R. Saha-Möller, J-aggregates: from serendipitous discovery to supramolecular engineering of functional dye materials, *Angew. Chem. Int. Ed Engl.*, 2011, **50**, 3376–3410.
83) R. Huenerbein and S. Grimme, Time-dependent density functional study of excimers and exciplexes of organic molecules, *Chem. Phys.*, 2008, **343**, 362–371.
84) M. Kołaski, C. R. Arunkumar and K. S. Kim, Aromatic Excimers: *Ab Initio* and TD-DFT Study, *J. Chem. Theory Comput.*, 2013, **9**, 847–856.
85) J. Hoche, M. Flock, X. Miao, L. N. Philipp, M. Wenzel, I. Fischer and R. Mitric, Excimer formation dynamics in the isolated tetracene dimer, *Chem. Sci.*, 2021, **12**, 11965–11975.
86) A. C. Hancock and L. Goerigk, Noncovalently bound excited-state dimers: a perspective on current time-dependent density functional theory approaches applied to aromatic excimer models, *RSC Adv.*, 2022, **12**, 13014–13034.
87) F. Muniz-Miranda, P. Minei, L. Contiero, F. Labat, I. Ciofini, C. Adamo, F. Bellina and A. Pucci, Aggregation Effects on Pigment Coatings: Pigment Red 179 as a Case Study, *ACS Omega*, 2019, **4**, 20315–20323.
88) A. Rosati, M. Fedel and S. Rossi, NIR reflective pigments for cool roof applications: A comprehensive review, *J. Clean. Prod.*, 2021, **313**, 127826.
89) V. Barone, J. Bloino, S. Monti, A. Pedone and G. Prampolini, Fluorescence spectra of organic dyes in solution: a time dependent multilevel approach, *Phys Chem Chem Phys*, 2011, **13**, 2160–2166.
90) V. Barone, R. Improta and N. Rega, Quantum Mechanical Computations and Spectroscopy: From Small Rigid Molecules in the Gas Phase to Large Flexible Molecules in Solution, *Acc. Chem. Res.*, 2008, **41**, 605–616.
91) C. A. Guido, D. Jacquemin, C. Adamo and B. Mennucci, Electronic Excitations in Solution: The Interplay between State Specific Approaches and a Time-Dependent Density Functional Theory Description, J. Chem. Theory Comput., 2015, 11, 5782–5790
92) C. Adamo and D. Jacquemin, The calculations of excited-state properties with Time-Dependent Density Functional Theory, Chem. Soc. Rev., 2013, 42, 845–856
93) D. Jacquemin, B. Mennucci and C. Adamo, Excited-state calculations with TD-DFT: from benchmarks to simulations in complex environments, Phys. Chem. Chem. Phys., 2011, 13, 16987
94) R. Sarkar, M. Boggio-Pasqua, P.-F. Loos and D. Jacquemin, Benchmarking TD-DFT and Wave Function Methods for Oscillator Strengths and Excited-State Dipole Moments, *J. Chem. Theory Comput.*, 2021, **17**, 1117–1132.
95) W. Liang, Z. Pei, Y. Mao and Y. Shao, Evaluation of molecular photophysical and photochemical properties using linear response time-dependent density functional theory with classical embedding: Successes and challenges, *J. Chem. Phys.*, 2022, **156**, 210901
96) J. Tomasi, B. Mennucci and R. Cammi, Quantum Mechanical Continuum Solvation Models, *Chem. Rev.*, 2005, **105**, 2999–3094.
97) B. Mennucci, Polarizable continuum model, *Wiley Interdiscip. Rev. Comput. Mol. Sci.*, 2012, **2**, 386–404.
98) A. Klamt, Conductor-like screening model for real solvents: A new approach to the quantitative calculation of solvation phenomena, *J. Phys. Chem.*, 1995, **99**, 2224–2235.
99) M. Cossi, N. Rega, G. Scalmani and V. Barone, Energies, structures, and electronic properties of

molecules in solution with the C-PCM solvation model, *J. Comput. Chem.*, 2003, **24**, 669–681.
100) S. Sharafy and K. Muszkat, Viscosity Dependence of Fluorescence Quantum Yields, *J. Am. Chem. Soc.*, 1971, **93**, 4119-.
101) G. Fischer, G. Seger, K. Muszkat and E. Fischer, Emissions of Sterically Hindered Stilbene Derivatives and Related Compounds .4. Large Conformational Differences Between Ground and Excited-States of Sterically Hindered Stilbenes - Implications Regarding Stokes Shifts and Viscosity or Temperature-Dependence of Fluorescence Yields, *J. Chem. Soc.-Perkin Trans. 2*, 1975, 1569–1576.
102) B. Wilhelmi, Influence of Solvent Viscosity on Excited-State Lifetime and Fluorescence Quantum Yield of Dye Molecules, *Chem. Phys.*, 1982, **66**, 351–355.
103) D. Todd and G. Fleming, Cis-Stilbene Isomerization - Temperature-Dependence and the Role of Mechanical Friction, *J. Chem. Phys.*, 1993, **98**, 269–279.
104) A. D. Kummer, C. Kompa, H. Niwa, T. Hirano, S. Kojima and M. E. Michel-Beyerle, Viscosity-dependent fluorescence decay of the GFP chromophore in solution due to fast internal conversion, *J. Phys. Chem. B*, 2002, **106**, 7554–7559.
105) R. Improta and V. Barone, Absorption and Fluorescence Spectra of Uracil in the Gas Phase and in Aqueous Solution: A TD-DFT Quantum Mechanical Study, *J. Am. Chem. Soc.*, 2004, **126**, 14320–14321.
106) L. Bernasconi, S. Tomić, M. Ferrero, M. Rérat, R. Orlando, R. Dovesi and N. M. Harrison, First-principles optical response of semiconductors and oxide materials, *Phys. Rev. B*, 2011, **83**, 195325.
107) M. Arhangelskis, D. B. Jochym, L. Bernasconi, T. Friščić, A. J. Morris and W. Jones, Time-Dependent Density-Functional Theory for Modeling Solid-State Fluorescence Emission of Organic Multicomponent Crystals, *J. Phys. Chem. A*, 2018, **122**, 7514–7521.
108) L. Le Bras, C. Adamo and A. Perrier, Modeling the Modulation of Emission Behavior in E/Z Isomers of Dipyrrolyldiphenylethene: From Molecules to Nanoaggregates, *J. Phys. Chem. C*, 2017, **121**, 25603–25616.
109) X. Zheng, Q. Peng, L. Zhu, Y. Xie, X. Huang and Z. Shuai, Unraveling the aggregation effect on amorphous phase AIE luminogens: a computational study, *Nanoscale*, 2016, **8**, 15173–15180.
110) G. Sun, Y. Zhao and W. Liang, Aggregation-Induced Emission Mechanism of Dimethoxy-Tetraphenylethylene in Water Solution: Molecular Dynamics and QM/MM Investigations, *J. Chem. Theory Comput.*, 2015, **11**, 2257–2267.
111) Y. Shigemitsu, T. Mutai, H. Houjou and K. Araki, Influence of intermolecular interactions on solid state luminescence of imidazopyridines: theoretical interpretations using FMO-TDDFT and ONIOM approaches, *Phys. Chem. Chem. Phys.*, 2014, **16**, 14388.
112) M. Rivera, M. Dommett and R. Crespo-Otero, ONIOM(QM:QM′) Electrostatic Embedding Schemes for Photochemistry in Molecular Crystals, *J. Chem. Theory Comput.*, 2019, **15**, 2504–2516.
113) M. Rivera, M. Dommett, A. Sidat, W. Rahim and R. Crespo-Otero, FROMAGE : A library for the study of molecular crystal excited states at the aggregate scale, *J. Comput. Chem.*, 2020, **41**, 1045–1058.
114) L. Wilbraham, C. Adamo, F. Labat and I. Ciofini, Electrostatic Embedding To Model the Impact of Environment on Photophysical Properties of Molecular Crystals: A Self-Consistent Charge Adjustment Procedure, *J. Chem. Theory Comput.*, 2016, **12**, 3316–3324.
115) L. Wilbraham, M. Louis, D. Alberga, A. Brosseau, R. Guillot, F. Ito, F. Labat, R. Métivier, C. Allain and I. Ciofini, Revealing the Origins of Mechanically Induced Fluorescence Changes in Organic Molecular Crystals, *Adv. Mater.*, 2018, **30**, 1800817.
116) D. Luise, L. Wilbraham, F. Labat and I. Ciofini, Modeling UV–Vis spectra of low dimensional materials using electrostatic embedding: The case of CdSe, *J. Comput. Chem.*, 2021, **42**, 1212–1224.
117) J. Su, D. Luise, I. Ciofini and F. Labat, Modeling the Electronic and Optical Properties of Lead-Based Perovskite Materials: Insights from Density Functional Theory and Electrostatic Embedding, *J. Phys. Chem. C*, 2023, acs.jpcc.2c08515.

118) S. J. Strickler and R. A. Berg, Relationship between Absorption Intensity and Fluorescence Lifetime of Molecules, *J. Chem. Phys.*, 1962, **37**, 814–822.
119) K. Asada, T. Kobayashi and H. Naito, Temperature dependence of photoluminescence in polyfluorene thin films—Huang–Rhys factors of as-coated, annealed and crystallized thin films, *Thin Solid Films*, 2006, **499**, 192–195.
120) J. Cornil, D. Beljonne, C. M. Heller, I. H. Campbell, B. K. Laurich, D. L. Smith, D. D. C. Bradley, K. Müllen and J. L. Brédas, Photoluminescence spectra of oligo-paraphenyllenevinylenes: a joint theoretical and experimental characterization, *Chem. Phys. Lett.*, 1997, **278**, 139–145.
121) K. Huang and A. Rhys, in *Selected Papers of Kun Huang*, WORLD SCIENTIFIC, 2000, vol. Volume 23, pp. 74–92.
122) K. Müller-Dethlefs and P. Hobza, Noncovalent Interactions: A Challenge for Experiment and Theory, *Chem. Rev.*, 2000, **100**, 143–168.
123) G. A. DiLabio and A. Otero-de-la-Roza, in *Reviews in Computational Chemistry*, eds. A. L. Parrill and K. B. Lipkowitz, John Wiley & Sons, Inc, Hoboken, NJ, 2016, pp. 1–97.
124) M. A. Izquierdo, J. Shi, S. Oh, S. Y. Park, B. Milián-Medina, J. Gierschner and D. Roca-Sanjuán, Excited-state non-radiative decay in stilbenoid compounds: an ab initio quantum-chemistry study on size and substituent effects, *Phys. Chem. Chem. Phys.*, 2019, **21**, 22429–22439.
125) X. Gao, Q. Peng, Y. Niu, D. Wang and Z. Shuai, Theoretical insight into the aggregation induced emission phenomena of diphenyldibenzofulvene: a nonadiabatic molecular dynamics study, Phys. Chem. Chem. Phys., 2012, 14, 14207–14216.
126) J. Peng, X. He, Y. Li, J. Guan, B. Wu, X. Li, Z. Yu, J. Liu and J. Zheng, Restriction of crossing conical intersections: the intrinsic mechanism of aggregation-induced emission, Phys. Chem. Chem. Phys., 2023, 25, 12342–12351.
127) W.-L. Ding, X.-L. Peng, G.-L. Cui, Z.-S. Li, L. Blancafort and Q.-S. Li, Potential-Energy Surface and Dynamics Simulation of THBDBA: An Annulated Tetraphenylethene Derivative Combining Aggregation-Induced Emission and Switch Behavior, ChemPhotoChem, 2019, 3, 814–824.
128) S. Gozem, F. Melaccio, A. Valentini, M. Filatov, M. Huix-Rotllant, N. Ferré, L. M. Frutos, C. Angeli, A. I. Krylov, A. A. Granovsky, R. Lindh and M. Olivucci, Shape of Multireference, Equation-of-Motion Coupled-Cluster, and Density Functional Theory Potential Energy Surfaces at a Conical Intersection, *J. Chem. Theory Comput.*, 2014, **10**, 3074–3084.
129) Q. Wu and W. Yang, Empirical correction to density functional theory for van der Waals interactions, *J. Chem. Phys.* 2002, **116**, 515–524.
130) J. Klimeš and A. Michaelides, Perspective: Advances and challenges in treating van der Waals dispersion forces in density functional theory, *J. Chem. Phys.*, 2012, **137**, 120901 20)
131) S. Grimme, Density functional theory with London dispersion corrections, *Wiley Interdiscip. Rev. Comput. Mol. Sci.*, 2011, **1**, 211–228.
132) D. Casanova and A. I. Krylov, Spin-flip methods in quantum chemistry, *Phys. Chem. Chem. Phys.*, 2020, **22**, 4326–4342.
133) M. Huix-Rotllant, A. Nikiforov, W. Thiel and M. Filatov, in *Density-Functional Methods for Excited States*, eds. N. Ferré, M. Filatov and M. Huix-Rotllant, Springer International Publishing, Cham, 2016, pp. 445–476.
134) É. Brémond, M. Savarese, N. Q. Su, Á. J. Pérez-Jiménez, X. Xu, J. C. Sancho-García and C. Adamo, Benchmarking Density Functionals on Structural Parameters of Small-/Medium-Sized Organic Molecules, J. Chem. Theory Comput., 2016, 12, 459–465
135) E. Brémond, M. Savarese, C. Adamo and D. Jacquemin, Accuracy of TD-DFT Geometries: A Fresh Look, J. Chem. Theory Comput., 2018, 14, 3715–3727.
136) J. Luo, Z. Xie, J. W. Y. Lam, L. Cheng, B. Z. Tang, H. Chen, C. Qiu, H. S. Kwok, X. Zhan, Y. Liu and D. Zhu, Aggregation-induced emission of 1-methyl-1,2,3,4,5-pentaphenylsilole, *Chem. Commun.*,

2001, 1740–1741.
137) C. Micheletti, Q. Wang, F. Ventura, M. Turelli, I. Ciofini, C. Adamo and A. Pucci, Red-emitting tetraphenylethylene derivative with aggregation-induced enhanced emission for luminescent solar concentrators: A combined experimental and density functional theory study, *Aggregate*, DOI:10.1002/agt2.188.
138) E. Bremond, M. Boggio-Pasqua, N. Leygue, M. Fodili, P. Hoffmann, N. Saffon-Merceron, R. Métivier and S. Fery-Forgues, ESIPT-active cinnamoyl pyrones are bright solid-state emitters: Revisited theoretical approach and experimental study, *Dyes Pigments*, 2023, **211**, 111046.
139) Z. Yang, Z. Chi, Z. Mao, Y. Zhang, S. Liu, J. Zhao, M. P. Aldred and Z. Chi, Recent advances in mechano-responsive luminescence of tetraphenylethylene derivatives with aggregation-induced emission properties, *Mater. Chem. Front.*, 2018, **2**, 861–890.
140) W. Chen, H. Chen, Y. Huang, Y. Tan, C. Tan, Y. Xie and J. Yin, Molecular Design and Photothermal Application of Thienoisoindigo Dyes with Aggregation-Induced Emission, *ACS Appl. Bio Mater.*, 2022, **5**, 3428–3437.
141) W.-L. Ding, X.-L. Peng, G.-L. Cui, Z.-S. Li, L. Blancafort and Q.-S. Li, Potential-Energy Surface and Dynamics Simulation of THBDBA: An Annulated Tetraphenylethene Derivative Combining Aggregation-Induced Emission and Switch Behavior, *ChemPhotoChem*, 2019, **3**, 814–824.
142) Y. Dong, J. W. Y. Lam, A. Qin, J. Liu, Z. Li, B. Z. Tang, J. Sun and H. S. Kwok, Aggregation-induced emissions of tetraphenylethene derivatives and their utilities as chemical vapor sensors and in organic light-emitting diodes, *Appl. Phys. Lett.*, 2007, **91**, 011111.
143) H. Stegemeyer, Luminescence of Sterically Hindered Arylethylenes, *Berichte Bunsenges. Für Phys. Chem.*, 1968, **72**, 335–340.
144) G. Fischer, E. Fischer and H. Stegemeyer, Fluorescence and Absorption Spectra of Sterically Hindered Arylethylenes in the Neat Glassy State, *Berichte Bunsenges. Für Phys. Chem.*, 1973, **77**, 685–687.
145) D. A. Shultz and M. A. Fox, Effect of phenyl ring torsional rigidity on the photophysical behavior of tetraphenylethylenes, *J. Am. Chem. Soc.*, 1989, **111**, 6311–6320.
146) J. Guan, R. Wei, A. Prlj, J. Peng, K.-H. Lin, J. Liu, H. Han, C. Corminboeuf, D. Zhao, Z. Yu and J. Zheng, Direct Observation of Aggregation-Induced Emission Mechanism, *Angew. Chem. Int. Ed.*, 2020, **59**, 14903–14909.
147) A. Prlj, N. Došlić and C. Corminboeuf, How does tetraphenylethylene relax from its excited states?, *Phys. Chem. Chem. Phys.*, 2016, **18**, 11606–11609.
148) M.-S. Yuan, D.-E. Wang, P. Xue, W. Wang, J.-C. Wang, Q. Tu, Z. Liu, Y. Liu, Y. Zhang and J. Wang, Fluorenone Organic Crystals: Two-Color Luminescence Switching and Reversible Phase Transformations between π–π Stacking-Directed Packing and Hydrogen Bond-Directed Packing, *Chem. Mater.*, 2014, **26**, 2467–2477.
149) M.-S. Yuan, X. Du, F. Xu, D.-E. Wang, W.-J. Wang, T.-B. Li, Q. Tu, Y. Zhang, Z. Du and J. Wang, Aggregation-induced bathochromic fluorescent enhancement for fluorenone dyes, *Dyes Pigments*, 2015, **123**, 355–362.
150) F. Xu, H. Wang, X. Du, W. Wang, D.-E. Wang, S. Chen, X. Han, N. Li, M.-S. Yuan and J. Wang, Structure, property and mechanism study of fluorenone-based AIE dyes, *Dyes Pigments*, 2016, **129**, 121–128.
151) S. Park, J. E. Kwon, S.-Y. Park, O.-H. Kwon, J. K. Kim, S.-J. Yoon, J. W. Chung, D. R. Whang, S. K. Park, D. K. Lee, D.-J. Jang, J. Gierschner and S. Y. Park, Crystallization-Induced Emission Enhancement and Amplified Spontaneous Emission from a CF_3 -Containing Excited-State Intramolecular-Proton-Transfer Molecule, *Adv. Opt. Mater.*, 2017, **5**, 1700353.
152) A. J. Stasyuk, P. J. Cywiński and D. T. Gryko, Excited-state intramolecular proton transfer in 2′-(2′-hydroxyphenyl)imidazo[1,2- a]pyridines, *J. Photochem. Photobiol. C Photochem. Rev.*, 2016, **28**,

116–137.
153) D. Göbel, D. Duvinage, T. Stauch and B. J. Nachtsheim, Nitrile-substituted 2-(oxazolinyl)-phenols: minimalistic excited-state intramolecular proton transfer (ESIPT)-based fluorophores, *J. Mater. Chem. C*, 2020, **8**, 9213–9225.
154) P. Zhou and K. Han, ESIPT-based AIE luminogens: Design strategies, applications, and mechanisms, *Aggregate*, DOI:10.1002/agt2.160.
155) D. J. Stewart, M. J. Dalton, R. N. Swiger, T. M. Cooper, J. E. Haley and L.-S. Tan, Exciplex Formation in Blended Spin-Cast Films of Fluorene-Linked Dyes and Bisphthalimide Quenchers, *J. Phys. Chem. A*, 2013, **117**, 3909–3917

Table of Contents Entry